CLM-P681

UKAEA

Preprint

TOKAMAK POWER BALANCES IN O-D

R. D. GILL

CULHAM LABORATORY
Abingdon Oxfordshire

1982

CLM-P 681

TOKAMAK POWER BALANCES IN O-D

R.D. Gill

Culham Laboratory, Abingdon, Oxon., OX14 3DB, UK
(Euratom/UKAEA Fusion Association)

ABSTRACT

Electron and ion empirical energy containment times derived from a range of machines are used to construct a O-D power balance model for tokamak discharges. The temperature dependence of the electron containment time is determined from the consideration of neutral injection heated discharges. The model is shown to be in excellent agreement with existing experiments both with and without injection heating and is applied to the next generation of tokamaks. Both the plasma density limit and the β saturation effect observed in high power injection heating experiments are well explained after the addition of radiation losses to the model.

(To be submitted to Nuclear Fusion)

September 1982

1. INTRODUCTION

One of the key questions in current tokamak research is the determination and understanding of the energy transport processes. One approach to the study of this problem has been the derivation of empirical expressions for the total energy confinement time (τ_E) in terms of the main parameters of the tokamak discharges[1,2]. This approach, based mainly on data from ohmically heated discharges, has led to several expressions for τ_E of which the so-called Alcator or Intor scaling is the best known[3]. These scaling laws may then be used to predict the behaviour of future tokamaks.

Because previous approaches have generally had to rely on data from ohmically heated plasmas, the connection between the confinement and heating of the plasma in these experiments has meant that this approach could not determine the temperature dependence of τ_E. Further, in discharges with additional heating, the relative magnitudes of the electron and ion temperatures (T_e and T_i) may be quite different from those encountered in ohmically heated discharges, making the application of the values of τ_E determined from ohmic discharges suspect. It is therefore desirable to examine the experimental data from both ohmically and neutral injection heated discharges to determine separately the scaling of the electron and ion containment times (τ_{Ee} and τ_{Ei}) and in particular to try to establish the temperature scaling of τ_{Ee}. Only if τ_{Ee} and τ_{Ei} scale in a similar way with tokamak parameters will it be reasonable to try to apply a single expression for τ_E to any discharge regardless of the relative values of T_e and T_i.

In Section 2 of this paper the scalings of the energy containment times are derived and in Section 3 these are used to construct a

0-D power balance model which is then applied to various tokamaks with and without injection heating,(Section 4). Future tokamaks are discussed in Section 5. Plasma radiation loss is added to the model in Section 6. and applied to the density limits and β saturation effects observed in DITE and ISX-B. Conclusions follow in Section 7.

2. DETERMINATION OF SCALING LAWS

In this section the scaling laws for τ_{Ei} and τ_{Ee} are derived. The law for τ_{Ei} is derived from the consideration of a 0-D power balance in ohmically and neutral injection heated discharges. The main results of this approach have been published elsewhere[4] and here a resumé of the approach is given.

The tokamak data set of Pfeiffer and Waltz[2] [PW hereafter] is then used to determine the scaling of τ_{Ee}. In this data set T_i is not always known and it is therefore calculated from the scaling law for τ_{Ei} and the electron-ion equilibriation power exchange term, Q_{ei}; τ_{Ee} is then calculated from τ_E. The scaling of the electron temperature is also determined for ohmically heated discharges.

2.1 Ion Losses in Ohmic Discharges

It has been well known for many years that the ion temperature in an ohmically heated discharge is well described by the Artsimovich expression[5] which is based on ion conduction losses with the ions in the plateau region of collisionality. In this section the calculations leading to this scaling law are repeated in order to clearly establish the assumptions required.

The ion thermal conduction coefficient in the plateau region is[6]

$$K_i^{pl} = \frac{3}{2}\left(\frac{\pi}{2}\right)^{1/2}\left(\frac{\kappa T_i}{m_i}\right)^{1/2}\frac{r}{R^2}\frac{B_\theta}{B_\phi}\rho_{i\phi}^2 \qquad (1)$$

where m_i is the ion mass, and B_θ and B_ϕ are the poloidal and toroidal magnetic fields. The tokamak major and minor radii are R and r. The Larmor radius in the toroidal field is

$$\rho_{i\phi} = \sqrt{2m_i\kappa T_i}/eB_\phi \qquad (2)$$

where e is the electronic charge and κ is Boltzmann's constant. Combining (1) and (2) gives (in mks units, T_i in eV)

$$K_i^{pl} = 3.84 \times 10^{-4}\,\frac{q\sqrt{A_i}\;T_i^{3/2}}{RB_\phi^2} \qquad (3)$$

where A_i is the atomic weight and q is the plasma safety factor.

The conduction loss at radius r may then be written as

$$P_L^i = -\,4\pi^2\,R\,r\,K_i\,n_i e\frac{\partial T_i}{\partial r} \qquad (4)$$

This is evaluated at r/a = 0.5 and assuming that $r\,\partial T/\partial r \approx \hat{T}_i/2$, $n_i = \bar{n}_e$, and $q = q_L/2$. The assumption that the safety factor is half the value at the limiter (q_L) is best justified at high values of q_L. At low values of q_L, $q(r/a = 0.5) \approx 1$ would probably be a

better assumption. However, overall, in the range q_L = 2-8 it appears that this approximation is a reasonable one. Hence

$$P_L^i = 6.07 \times 10^{-22} \frac{\bar{n}_e \sqrt{A_i}\, q_L\, \hat{T}_i^{5/2}}{B_\phi^2} \tag{5}$$

The heat input to the plasma ions may be determined from the expression for the electron-ion collision energy transfer term[7] for a hydrogen plasma

$$P_{ei} = 7.6 \times 10^{-34} \frac{n_i\, \ell n\Lambda\, (T_e - T_i)}{A_i\, T_e^{3/2}} \tag{6}$$

where $\ell n\, \Lambda$ is the Coulomb logarithm. The heat input to the ions over the central region is obtained by integrating (6)

$$P_{ei} = \int 2\pi R\, 2\pi\, r\, dr\, 7.6 \times 10^{-34} \frac{n_i^2\, \ell n\Lambda\, (T_e - T_i)}{A_i\, T_e^{3/2}} \tag{7}$$

This is evaluated making the usual approximation that $(T_e - T_i)/T_e^{3/2} \approx 0.29/T_i^{1/2}$ when $T_i << T_e$ and integrating from r/a = 0 to r/a = 0.5. It is assumed that $\hat{n}_i = 2\bar{n}_e$. Hence

$$P_{ei} = 2.97 \times 10^{-33}\, Ra^2\, \bar{n}_e^2\, \ell n\Lambda / \hat{T}_i^{1/2}\, A_i \tag{8}$$

where $\hat{T}_i$ denotes the peak ion temperature. Equating this expression with the conduction loss (4) and taking $\ell n\Lambda = 16$ gives the well known law

$$\hat{T}_i = 2.50 \times 10^{-6} \sqrt[3]{I B_\phi R^2 \bar{n}_e}/\sqrt{A_i} \qquad (9)$$

where I is the total plasma current. A plot of this expression against the experimental values of T_i for the PW data set[2] determines the best empirical value for the constant as 2.6×10^{-6} in excellent agreement with the value in equation (9).

Using this empirical value, the ion losses in the plateau region can be written as

$$P_i = 5.4 \times 10^{-22} \frac{\bar{n}_e \sqrt{A_i}\, q_L \hat{T}_i^{5/2}}{B_\phi^2} \qquad (10)$$

2.2 Ion Losses in Injection Heated Discharges

In neutral injection heated discharges there is an additional heat input to the ions from the injectors. In this section a simple model will be developed for determining the fraction of injection energy passing to the ions and electrons. A 0-D model of the ion transport will be constructed and applied to the analysis of high power injection heating experiments.

2.2.1 Beam penetration

Consider an injection system, with power P_{NI} and mean injection

energy E_f, which can be situated either radially or tangentially as shown in Figure 1. The tangential injectors are assumed to be tangential to major radius R - a/2. The variation of the plasma density is shown schematically. In order to estimate the effects of shine through and poor penetration on the injection energy deposition it is assumed that injection energy is deposited in the plasma if fast ions penetrate past the (R + a/2) point (Q) and is lost if they pass point C. The cross-section for beam ionisation is σ and is approximately temperature independent and therefore the shine through will be

$$P_{lost} = P_{NI} \exp\left(-\int_A^C n_e \sigma \, d\ell\right) \tag{11}$$

which can be approximated very crudely using the schematic density dependence to give

$$\begin{aligned} P_{lost}(\text{tangential}) &\approx P_{NI}\, e^{-\frac{5}{4}\bar{n}_e L \sigma} \\ P_{lost}(\text{radial}) &\approx P_{NI}\, e^{-2\bar{n}_e a \sigma} \end{aligned} \tag{12}$$

where $$L^2 = 4[(R + a)^2 - (R - a/2)^2]$$

It is further assumed that injected ions trapped between A and Q are unavailable for bulk plasma heating. The loss in this case is

$$P'_{Lost}(\text{tangential}) \approx P_{NI}(1 - e^{-\frac{1}{16}\bar{n}_e L\sigma})$$

$$P'_{Lost}(\text{radial}) \approx P_{NI}(1 - e^{-\frac{1}{4}\bar{n}_e a\sigma}) \qquad (13)$$

A more realistic model with density varying as $(1 - (r/a)^2)^2$ where a is the minor radius of the limiter suggests that the exponents in (13) should be reduced by a factor of 2 and these reduced values will be adopted. For the machines considered in this paper $L \approx 6.8a$ is adopted for determining this correction.

Of the beam power that is not lost, some will heat the ions, some the electrons, and some will be lost by charge exchange. Although the effects of charge exchange on the thermal ions will not be considered, it is necessary to include the effects of neutrals on the fast ions for realistic modelling. This is because at low plasma density loss of fast ions by charge exchange is a major power loss and if not included leads to a model in which increasingly high temperatures are attained at low density. Unfortunately, the plasma neutral density (n_o) is often only poorly determined. Values obtained for DITE agree very roughly with

$$n_o = 1.61 \times 10^{55}/\bar{n}_e^{2.1} \qquad (14)$$

This is assumed to scale to other machines as a^2 and hence

$$n_o = \frac{1.61 \times 10^{55}}{\bar{n}_e^{2.1}} \left(\frac{0.26}{a}\right)^2 \qquad (15)$$

It must be emphasised that in most of the calculations in this paper this correction is extremely small and our crude approach is quite acceptable.

2.2.2 Energy deposition by neutral beam

A population of fast ions with density n_f and energy E_f is slowed down in a plasma according to[8,9]

$$n_f \frac{dE_f}{dt} = - \frac{E_f}{\tau_s} - \frac{E_f}{\tau_s} \left(\frac{E_c}{E_f}\right)^{3/2} \tag{16}$$

where the critical energy

$$E_c = \kappa T_e \left\{ \frac{3\sqrt{\pi}\ A_f^{3/2} [Z]}{4\ A_e^{1/2}} \right\}^{2/3}, \quad [Z] = \frac{1}{n_e} \Sigma\ n_j\ Z_j^2/A_j \tag{17}$$

and

$$\tau_s = 3\pi\sqrt{2\pi}\ \frac{\varepsilon_o^2\ A_f\ (\kappa T_e)^{3/2}\ \sqrt{m_H}}{Z_f^2\ e^4\ \ell n\Lambda\ n_e\ A_e^{1/2}} \tag{18}$$

with A_f, A_j and A_e the atomic weights of the fast ions, plasma ions and the electrons; Z_f and Z_j are the atomic number of the injected ions and the other ions and m_H is the mass of the hydrogen atom; ε_o is the permittivity of free space.

In equation (16) the first term on the RHS represents power to the electrons; the second, power to the ions. The total power loss

from the fast ion population is given by

$$\frac{dW_f}{dt} = n_f \frac{dE_f}{dt} + E_f \frac{dn_f}{dt} = n_f \frac{dE_f}{dt} - n_f \frac{E_f}{\tau_{cx}} \qquad (19)$$

where $W_f = n_f E_f$ and τ_{cx} is the time for loss of fast ions by charge exchange on the plasma neutral atom gas. The time taken for the fast ions to slow down to thermal energies is

$$t_o = \frac{2\tau_s}{3} \ell n \left\{ \frac{E_f^{3/2} + E_c^{3/2}}{E_c^{3/2}} \right\} \qquad (20)$$

The fractions (f_e, f_i) of the fast ion power transferred to the electrons and ions can be calculated from (16) and (19) and are presented in a convenient form in ref[10] as functions of E_o/E_c and $2\tau_s/\tau_{cx}$. In this paper these values are used, evaluated at the average electron temperature which is taken as $(\hat{T}_e/2)$. $[Z]^{2/3}$ is always well approximated by unity.

In summary, the fraction of the beam power, P_{NI}, delivered to the electrons and ions is determined by evaluating the edge losses to give $f P_{NI}$ and then evaluating (f_e, f_i) to give the total power to the electrons and ions as $f f_{e,i} P_{NI}$ respectively.

2.2.3 Ion losses at low collisionality

Although plateau conduction losses are an adequate approximation when the plasma collisionality parameter ν_i^* is large, in injection

heated discharges, the ions are often well into the collisionless regime and it is then expected theoretically that the ion losses are much reduced[11]. For example, Hinton and Rosenbluth[12] show that in the banana-plateau regime the ion thermal conductivity

$$\frac{K_i}{K_i^{pl}} = 0.35 \frac{\nu_i^* (1 + 1.31\, \nu_i^*\, \delta^{3/2})}{(1 + 1.03\, \nu_i^{*1/2} + 0.185\, \nu_i^*)} \qquad (21)$$

where the superscript "pl" denotes the plateau value of K_i and $\delta = r/R$. In the banana regime the dependence of K_i on δ is rather weak and it is therefore assumed that, over a restricted range of ν_i^*, it is possible to write the ion thermal conductivity as

$$\frac{K_i}{K_i^{pl}} = a\, \nu_i^{*b} \qquad (22)$$

Combining this with the previous expression for the plateau ion losses[10] gives

$$P_{Loss} = a\, \bar{\nu}_i^{*b}\, P_i \qquad (23)$$

where the average collisionality parameter, $\bar{\nu}_i^*$, is found by evaluating

$$\nu_i^* = \left(\frac{R}{r}\right)^{3/2} \frac{q\, R}{v_i\, \tau_i} \qquad (24)$$

at r/a = 0.5 with an ion temperature $\hat{T}_i/2$. v_i and τ_i are the ion velocity and collision time with the latter evaluated by multiplying the hydrogenic collision time by $1/\sqrt{2}(Z_{eff} - 0.414)$.

The parameters a and b are derived from the consideration of the heating obtained in several high power neutral injection experiments as described in ref[4] where it was found that a = 0.46 ± 0.18 and b = 0.65 ± 0.15 so that $P_{LOSS} = f(\bar{\nu}_i^*)\ P_i$ with $f(\bar{\nu}_i^*) = 0.46\ \bar{\nu}_i^{*0.65}$. Because $f(\bar{\nu}_i^*) = 1$ at $\bar{\nu}_i^* = 3.3$ it is reasonable to determine the ion losses from equation (23) for $\bar{\nu}_i^* < 3.3$ and take just the plateau value P_i for $\bar{\nu}_i^* > 3.3$.

2.2.4 Determination of electron energy containment time

For a plasma in a steady state with total electron and ion energies W_e and W_i the total (τ_E), electron (τ_{Ee}) and ion (τ_{Ei}) energy containment times may be defined as

$$\frac{W_e + W_i}{\tau_E} = P = P_e + P_i \qquad (25)$$

$$\frac{W_e}{\tau_{Ee}} = P_e \qquad \frac{W_i}{\tau_{Ei}} = P_i \qquad (26)$$

where P is the total input power and P_e, P_i are the input powers to the separate electron and ion systems. For an ohmically heated tokamak P = VI where V is the plasma loop volts; $P_i = P_{ei}$ and $P_e = VI - P_{ei}$ where P_{ei} is the electron-ion equipartition energy exchange term and it is assumed that the ohmic input is all within r/a < 0.5. Hence

$$\tau_E = \frac{W_e + W_i}{VI} \tag{27}$$

and

$$\tau_{Ee} = \frac{W_e}{VI - P_{ei}} \qquad \tau_{Ei} = \frac{W_i}{P_{ei}} \tag{28}$$

In some papers[2] an energy containment time is defined as

$$\tau'_{Ee} = \frac{W_e}{VI} \tag{29}$$

which is stated to be the electron energy containment time. This is related to the previously defined containment time by

$$\tau'_{Ee} = \tau_{Ee} \frac{(VI - P_{ei})}{VI} \tag{30}$$

and the definitions of the two containment times are the same only when P_{ei} is small.

A further relation between the containment times can be written as

$$\frac{W_e + W_i}{\tau_E} = \frac{W_e}{\tau_{Ee}} + \frac{W_i}{\tau_{Ei}} \tag{31}$$

In ref[2] the scaling of τ'_{Ee} with tokamak parameters was determined for an extensive set of ohmically heated discharges. The neglect

of the ion losses (or equivalently P_{ei}) was justified on the ground that these losses are poorly understood and are anyway small in relation to the electron losses.

In this paper the effects of the ion losses will be applied as a correction to the data of ref[2] in order to determine the scaling of τ_{Ee} rather than τ'_{Ee}. For a particular ohmically heated discharge the values of τ_{Ei} and P_{ei} are used to determine the ion losses when T_i is not known experimentally. The total plasma energy is determined from the mean density ($\bar{n}_i = \bar{n}_e$) and peak temperature ($\hat{T}_i$) assuming that the profiles vary as $(1 - (r/a)^2)^2$. Hence

$$W_i = 1.9 \times 10^{-18} \bar{n}_e \hat{T}_i a^2 R \qquad (32)$$

The data set of ref[2] is used to determine τ_{Ee} after applying a correction to τ'_{Ee} based on the values of τ_{Ei}, T_i
In most discharges this correction is relatively small and its accuracy is unimportant. The scaling of τ_{Ee} is then found by fitting a function of the form:

$$\tau_{Ee} = e^{a_0} A_i^{a_1} R^{a_2} a^{a_3} B^{a_4} I^{a_5} \bar{n}_e^{a_6} Z_e^{a_7} \qquad (33)$$

to the experimental data. A linear regression code determines the best values for $a_1 - a_7$.

As is well known, because of coupling between heating and containment in ohmically heated discharges the temperature dependence of τ_{Ee} cannot be determined by this method and T_e is therefore not included as a parameter in (33). From the initial fit it is clear that τ_{Ee} has no significant dependence on certain parameters and the least significant variable is removed and a new fit carried out. A statistical F test then showed if the removal of that variable statistically justified. This procedure is continued giving the best fit for τ_{Ee} as

$$\tau_{Ee} = e^{-63.4 \pm 0.4} \; R^{1.54 \pm 0.24} \; a^{0.75 \pm 0.15}$$

$$x \; \langle n_e \rangle^{1.33 \pm 0.06} \; Z_e^{0.35 \pm 0.1} \qquad (34)$$

The variables A_i, I and B have all been removed and $\langle n_e \rangle$ is defined as

$$\langle n_e \rangle = \frac{2}{a^2} \int_o^a n_e \; r \; dr \qquad (35)$$

Later in this paper it is assumed $\langle n_e \rangle \approx 0.75 \; \bar{n}_e$.

A similar procedure is followed to determine the temperature scaling for ohmically heated discharges with the result that

$$\hat{T}_e^p = e^{-5.04 \pm 0.46} \; R^{0.96 \pm 0.12} \; a^{-1.24 \pm 0.13} \; I^{0.81 \pm 0.05} \; Z_e^{0.37 \pm 0.05} \qquad (36)$$

in good agreement with equation (40) of ref[2].

The final form for the energy confinement time including the unknown temperature dependence is then

$$\tau_E^e = e^{-63.4} \; R^{1.54} \; a^{0.75} \; \langle n_e \rangle^{1.33} \; Z_e^{0.35} \left(\frac{\hat{T}_e}{\hat{T}_e^P} \right)^{\gamma_e} \qquad (37)$$

where γ_e has been determined from neutral injection heating experiments[4] to be 0.75 ± 0.20 (see section 3.2).

3. CONSTRUCTION OF 0-D MODEL

In this section a 0-D model for the time independent power balance for $r/a < 0.5$ is constructed first with ohmic heating alone and then also including neutral injection heating. Thermonuclear power production and Bremsstrahlung radiation losses are also added.

3.1 Ohmic Heating

Using the values of τ_{Ee}, τ_{Ei} and W_e, W_i from the previous sections it is possible to construct a 0-D model described by the following equations

$$\begin{aligned} VI - P_{ei} &= W_e/\tau_{Ee} \\ P_{ei} &= W_i/\tau_{Ei} \end{aligned} \qquad (38)$$

The values of W_e, W_i given by equation (32) are checked against the values of the PW data set and found to be in excellent agreement on average. The plasma loop volts, V, is also determined from the PW data set with the result that

$$V = 7.23 \times 10^{-3} \frac{I\ R\ Z_{eff}}{T_e^{3/2}\ a^2} \qquad (39)$$

The value of P_{ei} is determined by equation (8).

3.2 Ohmic plus Injection Heating

When neutral injection heating is present equations (38) for the power balances become

$$\begin{aligned} P_{NI}^{e} + VI - P_{ei} &= W_e/\tau_{Ee} \\ P_{NI}^{i} + P_{ei} &= W_i/\tau_{Ei} \end{aligned} \qquad (40)$$

Where τ_{Ee} must now include the unknown temperature dependence given by equation (37) and $P_{NI}^{e,i} = f\ f_{e,i}\ P_{NI}$. The value of the temperature exponent γ_e is determined by calculating T_e and T_i for the data set of ref[4] with various values of γ_e. The best overall fit (Figure 2) determines $\gamma_e = 0.75$ albeit with no great accuracy - (25% is estimated). However, plots similar to Figure 2 for different values of γ_e clearly exclude values as high as 1 or smaller than 0.5.

3.3 Addition of Thermo-nuclear Power and Bremsstrahlung

In order to extend the 0-D model to discuss tokamaks operating in or close to the reactor regime it is necessary to include Bremsstrahlung losses and thermo-nuclear power generation in the power balance equations. The model will be restricted to the consideration 100% D or 50 : 50 D-T plasma and it is assumed that the charged reaction products either escape giving no energy to the plasma or give their energy entirely to the plasma electrons. This latter assumption is rather approximate.

The power balance equations become

$$P_N + P_{NI}^e + VI - P_{ei} - P_B = \frac{W_e}{\tau_{Ee}} \qquad (41)$$

$$P_{NI}^e + P_{ei} = \frac{W_i}{\tau_{Ei}}$$

For a D-T plasma it is assumed that the ion losses are approximately determined by equation (10) with $A_i = 2.5$.

The Bremsstrahlung term is

$$P_B = \int_o^{a/2} 2\pi R \; 2\pi r \, dr \times 1.69 \times 10^{-38} \, n_e^2 \, T_e^{1/2} \qquad (42)$$

$$= 1.82 \times 10^{-37} \, Ra^2 \, \bar{n}_e^2 \, \hat{T}_e^{1/2}$$

for profiles which vary with $(1 - (r/a)^2)^2$.

The thermo-nuclear power produced per unit volume is

$$\gamma_T \frac{n_e^2}{4} \langle\sigma v\rangle Q \qquad (43)$$

where Q is the reaction energy and $\gamma_T = 2$ for the D-D plasma and 1 for the D-T plasma. The nuclear reaction rate $\langle\sigma v\rangle \approx \alpha_R T_i^{2.5}$ in the regions of interest giving for the integrated nuclear power

$$P_N = 0.20\pi^2 \gamma_T \alpha_R Q Ra^2 \bar{n}_e^2 T_i^{2.5} \qquad (44)$$

or

$$P_N = 0.20\pi^2 \gamma_T \langle\sigma v\rangle Q Ra^2 \bar{n}_e^2$$

The second expression for P_N is used in the model with values of $\langle\sigma v\rangle$ taken from Miley[13] using the analytic form given by Hively[14].

3.4 Summary

A 0-D model is constructed to give the best values of τ_{Ee} and T_i for both ohmically heated discharges at various densities and injection heated discharges at low density for a wide range of machines. At higher densities it is not easy to identify the separate losses of the ions and electrons but it will be asssumed that the model applies at all densities for any combination of injection and ohmic heating.

The main features of the plasma energy loss processes are now summarised. The electron energy containment time is

$$\tau_{Ee} = 2.00 \times 10^{-28} \; R^{1.54} \; a^{0.75} \; \bar{n}_e^{1.33} \; Z_{eff}^{0.35} \left(\frac{T_e}{\hat{T}_e^{P}}\right)^{\gamma_e} \qquad (45)$$

where $\gamma_e = 0$ for ohmic discharges and is otherwise 0.75. The predicted temperature for ohmic discharges is

$$\hat{T}_e^{P} = 6.47 \times 10^{-3} \; R^{0.96} \; I^{0.81} \; Z^{0.37}/a^{1.24} \qquad (46)$$

The electron total energy and power loss are

$$W_e = 1.9 \times 10^{-18} \; \bar{n}_e \; \hat{T}_e \; a^2 R \qquad (47)$$

$$P_e = 2.17 \times 10^{8} \frac{T_e^{0.25} \; a^{0.32} \; R^{0.18} \; I^{0.608}}{\bar{n}_e^{0.33} \; Z_{eff}^{0.06}} \qquad (48)$$

For the ions the containment time is

$$\tau_{Ei} = 3.52 \times 10^{3} \; \frac{Ra^2 \; B_\phi^2}{T_i^{3/2} \; q_L \; \sqrt{A_i}} \; \frac{1}{f(\nu_i^*)} \qquad (49)$$

with $f(\bar{\nu}_i^*) = 1$ for $\bar{\nu}_i^* > 3.3$ and $f(\bar{\nu}_i^*) = 0.46\ \bar{\nu}_i^{*\,0.65}$ when $\bar{\nu}_i^* < 3.3$.

The collisionality parameter $\bar{\nu}_i^*$ is

$$\bar{\nu}_i^* = 3.49 \times 10^{-16} \left(\frac{R}{a}\right)^{3/2} \frac{\bar{n}_e\, q_L\, R}{T_i^{\,2}}\, Z_{ION} \qquad (50)$$

with $$Z_{ION} = \sqrt{2}(Z_{eff} - 0.41)$$

For $\bar{\nu}_i^* < 3.3$ equation (49) can be rewritten as

$$\tau_{Ei} = 8.53 \times 10^{13} \frac{a^{2.97}\, B_\phi^{\,2}}{\bar{n}_e^{\,0.65}\, T_i^{\,0.20}\, A_i^{\,0.5}\, q_L^{\,1.65}\, R^{0.625}\, Z_{ION}^{0.65}} \qquad (51)$$

The expression for the ion total energy is similar to expression (47) and the ion power loss is

$$P_i = 5.4 \times 10^{-22} \cdot \frac{\bar{n}_e \sqrt{A_i}\, q_L\, \hat{T}_i^{5/2}}{B_\phi^2} f(\nu_i^*) \qquad (52)$$

or, for $\bar{\nu}_i^* < 3.3$

$$P_i = 2.22 \times 10^{-32} \frac{\bar{n}_e^{\,1.6}\, A_i^{\,0.5}\, q_L^{\,1.65}\, \hat{T}_i^{\,1.20}\, R^{1.625}\, Z_{ION}^{0.65}}{B_\phi^2\, a^{0.97}} \qquad (53)$$

4. APPLICATION TO VARIOUS MACHINES

Although the 0-D model is based on the analysis of results from many machines and the temperature and containment times given by the

model must in principle agree with experiment, it is interesting to see how well this operates in particular cases. One area of particular interest is the behaviour of τ_E in high field, high density experiments where deviations from $\tau_E \propto \bar{n}_e\ a^2$ scaling have been attributed to ion conduction plateau losses. Another area of interest is in the prediction of the density dependence of the ion temperature attained in neutral injection heating experiments. Excellent agreement is found between experiment and the 0-D model.

4.1 Alcator A Machine

Early experiments on the Alcator-A experiment[3] established the so called Alcator scaling for the total energy containment time $\tau_E = 4 \times 10^{-21}\ \bar{n}_e\ a^2$. The 0-D model has separate expressions for τ_{Ee} and τ_{Ei} and it is not clear that these are compatible with the Alcator scaling. The 0-D model has therefore been used with the parameters of Table 1 to calculate τ_E as a function of $\bar{n}_e$. The results, together with the experimental data[3] are shown in Figure 3. It can be seen that these are in excellent agreement except at the highest densities where the calculated values fall below experiment. The relative contribution to the power balance of the electron (P_e) and ion losses (P_i) shows (Figure 4) that ion losses predominate at high density (where the ion losses reach 70%). Further, the calculated electron and ion temperatures are in good agreement with experiment (Figure 5). The conclusion to be drawn is that the 0-D model is in good agreement with the experimental data but does not support the use of the simple na^2 scaling for τ_E.

4.2 Alcator C Machine

In Alcator C a very clear deviation from na^2 scaling was observed experimentally[15] and this is reproduced quite well by the model which shows roughly na^2 scaling at low density but with τ_E tending to saturate as higher densities are reached. The experimental points (Figure 6) actually fall a little below the calculated curve (which uses Table 1 data). Again, at high density the losses are mainly (80%) through the ion channel.

4.3 FT Machine

This machine is considerably larger than Alcator A or C and this leads to reduced ion losses and a reduced tendency for τ_E to saturate with increased density. The experimental points[16] and the calculated values agree with this (Figure 7) although there is quite a wide variation of the experimental values. The power balances show a reduced fraction of ion conduction loss which reaches a maximum of 60%. In addition the mean electron temperature is in reasonable agreement with the model (Figure 8).

4.4 PLT Machine

Experimental data on the ion temperatures attained during intense beam heating as a function of density have been presented for several combinations of plasma and beam and at several power levels[17] as shown in Figure 9.

The calculated values of T_i for each data set (see Table 1) are not too different and a band of 0-D model values can be put on the graph. These are in good agreement with experiment except at the lowest density where the calculations fall some 30% below experiment.

4.5 PDX

The PDX machine is quite similar in its main parameters to PLT except that radial rather than tangential neutral injection is used. One of the features of the injection heating results[18] has been the observation that the maximum ion temperature attained for a given injection power is dependent on the plasma current with the maximum temperatures comparable with those attained on PLT. These results are well predicted by the 0-D model and in Figure 10 the ion temperature is plotted as a function of $P_{abs}/\bar{n}_e$ where P_{abs} is the neutral injection power trapped by the plasma. In Figure 11 a comparison is made with the experimental data for I = 470 and 225kA. The calculations are for D^o injection into an H plasma. The experiment is in reasonable agreement with the calculations especially for the 225kA data. The electron temperatures are generally calculated to be larger than observed and in this respect, within the framework of the 0-D model, it would seem that there is a difference in the heating behaviour of PDX with 7MW of injection compared with PLT with 2MW of injection.

5. APPLICATION TO FUTURE MACHINES

Part of the purpose of developing a 0-D model is to try to predict the performance of future tokamak machines. In this section the predicted performance of JET, TFTR, INTOR and STARFIRE is presented. One of the difficulties of these calculations is to determine the maximum density at which a particular machine will

operate. With existing tokamaks it has been shown[19] that at moderately large values of q the maximum attainable density, for ohmically heated discharges is

$$\bar{n}_e(\max) = 2.3 \times 10^{20} \frac{\zeta B_\phi}{qR} \text{ with } \zeta = 1 \qquad (54)$$

It has been observed that this maximum can be increased[20] at low q by the application of powerful supplementary heating. All the calculations of this section will therefore be done with ζ = 1 and 4, representing pessimistic and optimistic views on the density which will be reached in a particular machine.

5.1 JET

The main parameters of JET[21] required as input to the model are listed in Table 1 for circularly cross-sectioned plasmas. In order to assess the overall potential of JET to achieve ignition the Lawson parameter $\bar{n}_e\tau_E$ is plotted as a function of temperature for ζ = 1 and 4 on Figure 12. The calculations assume $T_e = T_i$ and at high temperatures the calculated total poloidal β_θ increases above R/a which is thought to be the limit on β_θ. Above this limit the curves therefore become broken.

Also plotted on Figure 12 is the total power loss from the thermal plasma assuming that the charged components from the thermonuclear reactions either all escape (full line) or are all retained to heat the plasma (broken line).

The model therefore shows that JET will not reach ignition in circularly cross-sectioned plasmas. If improved values of $\bar{n}_e\tau_E$

are attained in D shaped plasmas then it may be possible to reach ignition. Input power levels in the region of 20-30MW of effective heating power coupled into the plasma will be required even to approach ignition.

JET will be heated by neutral injectors operating with D_2 at 160keV. The calculated values of T_e, T_i, $\bar{n}_e\tau_E$ and β_θ assuming the reaction products heat the plasma are shown in Figures 13 and 14 for 10 and 25MW of incident power for the parameters listed in Table 1. The density limits are at 7.8×10^{19} m^{-3} and 3.1×10^{20} m^{-3} for $\zeta = 1$ and 4 respectively. The rapid drop in temperature above $\bar{n}_e = 10^{20}$ m^{-3} is due to the inability of the neutral beams to penetrate the plasma and heat its centre. At an injection power of 25MW the closest approach to ignition occurs at $\bar{n}_e = 10^{20}$ m^{-3}, $T_e = T_i = 15$keV and $\bar{n}_e\tau_E = 10^{20}$ $m^{-3}s$. However, at 25MW the model predicts maximum β_θ values which would almost certainly not be achieved in practice because of MHD limitations.

5.2 Other Machines

The potential for reaching ignition of other machines being built (TFTR) or being planned (INTOR, STARFIRE) at present is shown in Figure 15 where $\bar{n}_e\tau_E$ is plotted versus $\bar{n}_e$. The parameters input to the model are in Table 1. The dotted curves again show the regions for which $\beta_\theta > R/a$. It appears that STARFIRE would ignite even if no increase in operating density could be obtained ($\zeta = 1$). Of the other machines, it appears that TFTR and INTOR might just get to ignition. The effective input power required (most of which would be supplied by additional heating) to get to or close to ignition is 12-25MW for STARFIRE, 10-30MW for TFTR, 10-25MW for INTOR and up to 30MW for JET.

6. ROLE OF RADIATION

One important omission from the 0-D model is the treatment of radiation loss. The fact that the expression for τ_{Ee} varies with density in a quite different way from that expected for a plasma dominated by impurity radiation losses implies that radiation losses generally play only a reduced role in determining the overall energy losses. However, it is also clear that as the plasma density increases radiation losses should become important as they increase as $n_e n_z$ with n_z the impurity density.

Ideally, expressions for the scaling of τ_{Ee} should be derived which have already been corrected to exclude the effects of radiation and these should then be used in a 0-D model which treats radiation separately. However, this approach is not possible at present because of a lack of a suitable data base and therefore to investigate the possible effects of radiation , the radiative power loss has just been added to the other losses as discussed below.

6.1 Radiation Model

It is assumed that the plasma contains only two impurity species, oxygen and iron which should be representative of both light and heavy metallic impurities. Radiation loss from the oxygen will generally contribute very little to the overall power balance in the central region. Consider a plasma with species with charge Z_i. The plasma effective charge is

$$Z_{eff} = \frac{1}{n_e} \Sigma\, n_i Z_i^2 \qquad (55)$$

with

$$n_e = \Sigma\, n_i Z_i$$

and the radiated power is

$$P_r = \Sigma\, n_e n_i\, f_i(T_e) \qquad (56)$$

where f_i depends only on the atomic physics of the impurity and, the electron temperature. Values of f_i are given for a coronal equilibrium model by ref[22]. For only two impurities

$$P_r = n_e n_p\, f_p(T_e) + n_e n_o\, f_o(T_e) + n_e n_{Fe}\, f_{Fe}(T_e) \qquad (57)$$

where the first term is just the bremsstrahlung radiation. In the 0-D model this expression is evaluated at the mean densities. The ratio of iron to oxygen atoms must be input to the model as

$$\gamma = \frac{n_{Fe}}{n_o} \qquad (58)$$

and then their absolute values are determined from the value of $\bar{n}_e$ and Z_{eff} using equation (55).

6.2 Effects of Addition of Radiation

Because P_r increases with density and decreases as a strong function of temperature the situation can arise in high density tokamak plasmas whereby a small increase in density produces an

increased radiative loss which cannot be compensated by a change in temperature. A situation is then created in which the plasma cannot be sustained by the applied input power. This process is illustrated schematically in Figure 16 where temperature is plotted versus density for a particular power input. It is quite clear that portion AB of the curve is unstable and that points approaching A on the upper part of the curve are also unstable. An increase in the power applied to the system would have the effect of increasing the range of temperature and density available. With no radiated power loss the temperature would just decrease as $\bar{n}_e$ increases, but with no region of instability.

Because only the radiation from Fe will contribute substantially to the overall power loss, the position of point A, that is the maximum attainable density, will vary with parameter γ.

6.2.1 Density and β-limits in DITE

Recent experiments[1.] on DITE have investigated both the maximum β and density attainable with high powered neutral injection heating. These experiments clearly showed that β did not increase linearly with injection power, as expected for $\bar{n}_e a^2$ energy containment time scaling and also that the range of operating density could be increased above the ohmic value by up to ~ 80% by the application of up to 1MW of additional heating.

With the parameters of Table 1 the range of T_e values calculated from the 0-D model are shown in Figure 17 for an iron/oxygen ratio of $\gamma = 0.2$. This value is reasonable in relation to impurity concentrations observed for other sets of DITE discharges[23]. The curves clearly show a density limit at ~ 1.02×10^{20} m^{-3} at injection input power of 800kW but a limit of 0.75×10^{20} at $P_{NI} = 0$.

Because the experimental data shows a density enhancement with injection of up to a factor of 2 with densities with and without injection of 8 and 4 x 10^{20} m^{-3} only in principle agreement can be claimed. The model cannot explain the failure to produce density enhancement at high q values and it can be only speculated that this may be due to poor containment of the fast ions in the system. The density operation diagram for DITE is shown schematically in Figure 18. Detailed agreement cannot be claimed nor even expected without a knowledge of γ and its variation with density. As the plasma current increases it becomes increasing MHD unstable and prevents the attainment of low values of q. These effects are not included in our model and this is seen in the linear increase in operating density with 1/q, in disagreement with experiment above $1/q \sim 0.3$.

The mean plasma β (Figure 19) clearly shows saturation as a function of density and the calculated curves are in reasonable agreement with experiment (Figure 14 of ref 19) although some of the details of the calculated curves are not reproduced by experiment. However, the maximum predicted β of $\sim$0.65% at 800kW is in reasonable agreement with the experimental value of $\sim$ 0.8% at 860kW.

It is instructive to examine the plasma energy balances as a function of density both with and without injection. The relative power losses via the electrons, ions or radiation are shown in Figure 20. In both cases it can be seen that radiation loss becomes important as the density limit is approached. The ion losses are very much more important in the injection heated discharges.

6.2.2 Density and β-limits in ISX-B

A similar calculation for the ISX-B experiment with γ = 0.3

shows very similar effects to DITE with a maximum β (excluding the fast ions) of 3.5% with 2.5MW of injection power compared with the observed[24] 3.5% (Figure 21). The observed maximum density of 1.0 x 10^{20} is also well reproduced by the calculations. The energy balances (Figure 22) show that for ISX-B, in contrast to DITE, radiation loss does not play a dominant role in high density injection heated discharges as ion losses predominate. In ohmically heated high density discharges radiation losses are important.

Again there are several details of the predictions which do not agree with the experiment, but the overall trends of the experimental data are in good agreement.

7. CONCLUSIONS

The main conclusions of this paper are:

i) An expression is obtained for the ion energy containment time valid over a large range of collisionality.

ii) An expression is obtained for the electron energy containment time including its temperature dependence.

iii) These containment times are used to construct a 0-D power balance model which allows for both ohmic and neutral injection heating methods.

iv) The model is successfully applied to the results from various tokamaks, some of which are in the original data set, some not.

v) The model is applied to future machines and predictions are made as to which of these will reach ignition.

vi) After adding radiation losses to the model, it is shown that the plasma β and density limits observed in recent experiments can be adequately explained.

TABLE 1

Parameters used in 0-D calculations

Machine	R (m)	a (m)	B_ϕ (T)	q	Z_{eff}	A_i (mu)	γ	A_f (mu)	E_f (keV)
Alcator A	0.54	0.095	6.7	5.09	1	1,2			
Alcator C	0.64	0.16	6	3.1	1.2	1			
FT	0.83	0.23	8	6.1	1	2			
PLT	1.3	0.4	3.2	4.3-5.1	3.5-5.1	1.2		2.1	40
PDX	1.43	0.44	2.2	3.2	3-6	1		2	50
JET	2.96	1.25	3.5	3.5	1.5	2,3		2	160
TFTR	2.48	0.85	6.0	3.5	1.5	2,3			
INTOR	5.2	1.3	5.5	3.5	1.5	2,3			
STARFIRE	7.0	1.94	5.8	3.5	1.5	2,3			
DITE	1.17	0.26	1.35	2.5	1.5	2	0.2	1	25
ISX-B	0.93	0.27	1.18	2.5	2	2	0.3	1	40

REFERENCES

1. Hugill, J. and Sheffield J., Nuclear Fusion 18 (1978) 15.

2. Pfeiffer, W. and Waltz, R.E., Nuclear Fusion 19 (1979) 51.

3. Apgar, E., Coppi, B., Gondhalekar, A., Helva, H., et al., Plasma Physics and Controlled Nuclear Fusion Research, 1976. 1 (1977) 247. IAEA, Vienna.

4. Gill, R.D., Physics Letters, to be published.

5. Artsimovich, L.A., Nuclear Fusion 12 (1972) 215.

6. Galeev, A.A. and Sagdeev, R.Z., JETP 26 (1968) 233.

7. Spitzer, L., "Physics of Fully Ionised Gases", 1962. Interscience Publishers, New York.

8. Stix, T.H., Plasma Physics 14 (1972) 367.

9. Callen, J.D., Colchin, R.J., Fowler, R.H., McAlees, D.G. et al., Plasma Physics and Controlled Fusion, 1974 1 (1975) 645. IAEA Vienna.

10. Berry, L.A., Symposium on Plasma Heating in Toroidal Devices, (1974) 151. Editrice Compositori, Bologna.

11. Hazeltine, F.L. and Hinton, R., Reviews of Modern Physics 48 (1976) 239.

12. Hinton, F.L. and Rosenbluth, M.N., Physics of Fluids 16 (1973) 836.

13. Miley, G.H., Towner, H. and Ivich, N., Report COO-2218-17, (1974) University of Illinois.

14. Hively, L.M., Nuclear Fusion 17 (1977) 873.

15. Fairfax, S., Gondhalekar, A., Granetz, R., Greenwald, M., et al., Plasma Physics and Controlled Nuclear Fusion Research 1980. 1 (1981) 439. IAEA Vienna.

16. Alladio, F., Bardotti, G., Bartiromo, R., Buceti, G. et al., Proceeding of the 10th European Conference on Controlled Fusion and Plasma Physics Moscow. 1 (1981) A-2.

17. Eubank, H., Goldston, R.J., Arunasalam, V., Bitter, M. et al., Plasma Physics and Controlled Nuclear Fusion Research, 1978. 1 (1979) 167 IAEA Vienna.

    Eubank, H., Goldston, R.J., Arunasalam, V., Bitter, M. et al., Physical Review Letters 43 (1979) 270.

18. Hawryluk, R.J., Arunasalam, V., Bell, M., Bitter, M., et al., Physical Review Letters 49 (1982) 326.

19. Hugill, J., Lomas, P.J., Wootton, A.J., Axon, K.B., et al., Nuclear Fusion, submitted for publication.

20. Axon, K.B., Clark, W.H.M., Cordey, J.G., Cox, M., et al. Plasma Physics and Controlled Nuclear Fusion Research, 1980 1 (1981) 413. IAEA Vienna.

21. The JET Proposal, EUR-JET-R5, (1975) CEC.

22. Post, D.E., Jensen, R.V., Tartar, C.B., Grasberger, W.H. and Lokke, W.A., Atomic Data and Nuclear Data Tables 20 (1977) 397.

23. Peacock, N.J., Hughes, M.H., Summers, H.P., Hobby, M., et al., Plasma Physics and Controlled Nuclear Fusion Research, 1978 1 (1979) 303. IAEA Vienna.

24. Swain, D.W., Murakami, M., Bates, S.C., Bush, C.E., et al., Nuclear Fusion 11 (1981) 1409.

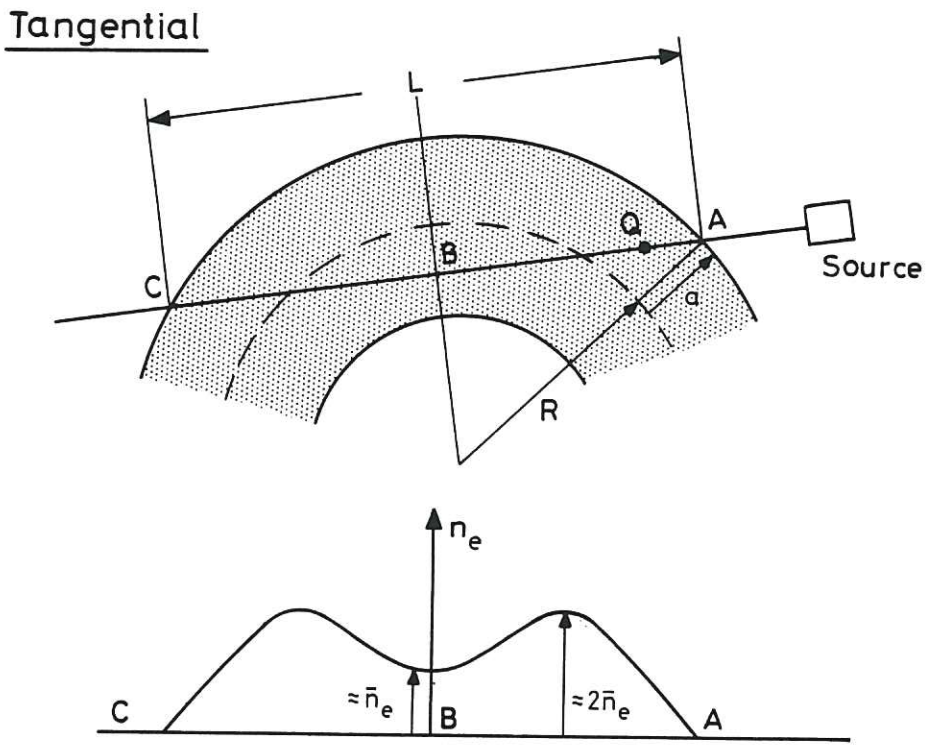

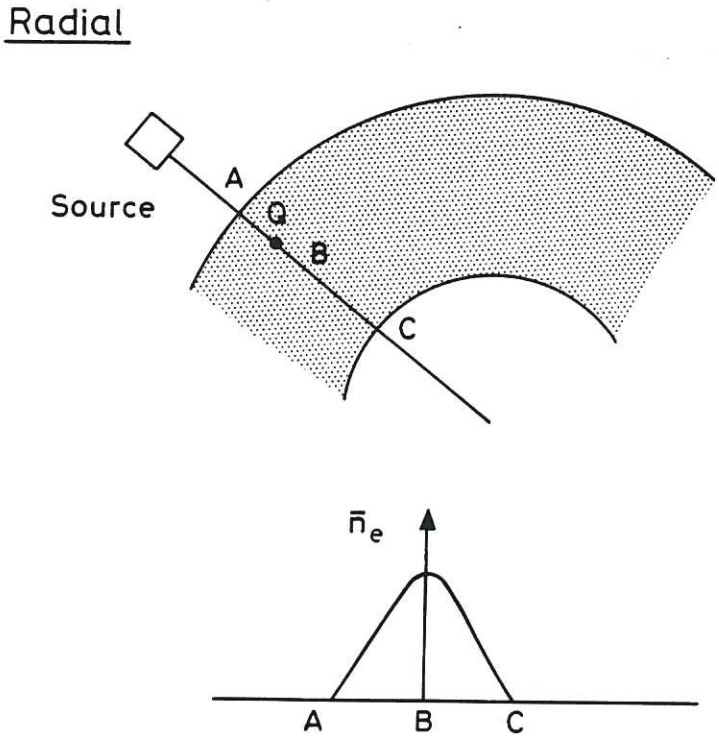

Fig.1 Geometrical arrangement of neutral injection heating systems for tangential and radial injection.

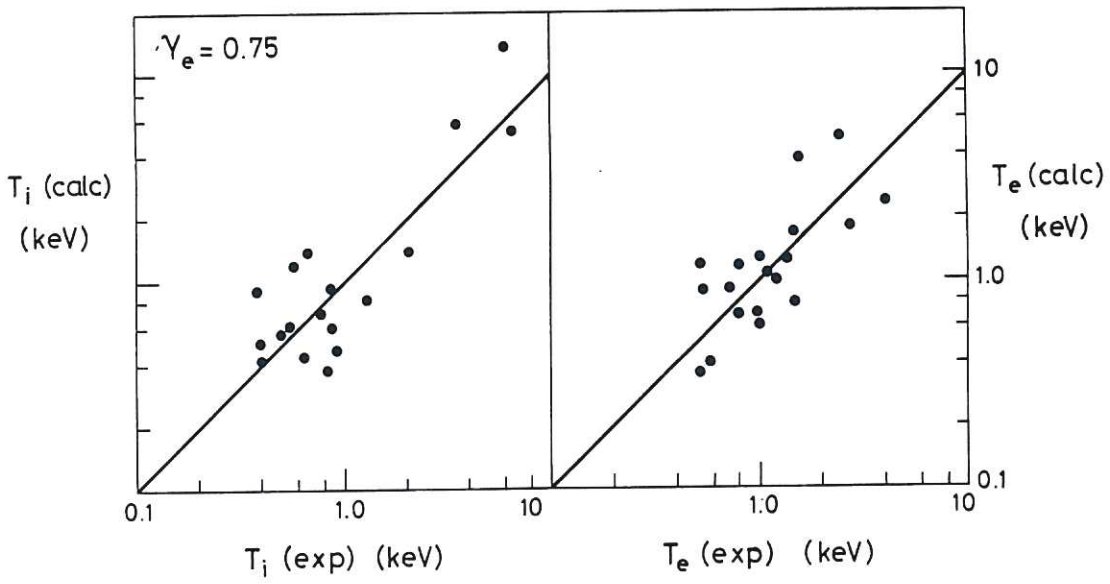

Fig.2 Comparison between calculated and experimental ion and electron temperatures for the data set of ref.4).

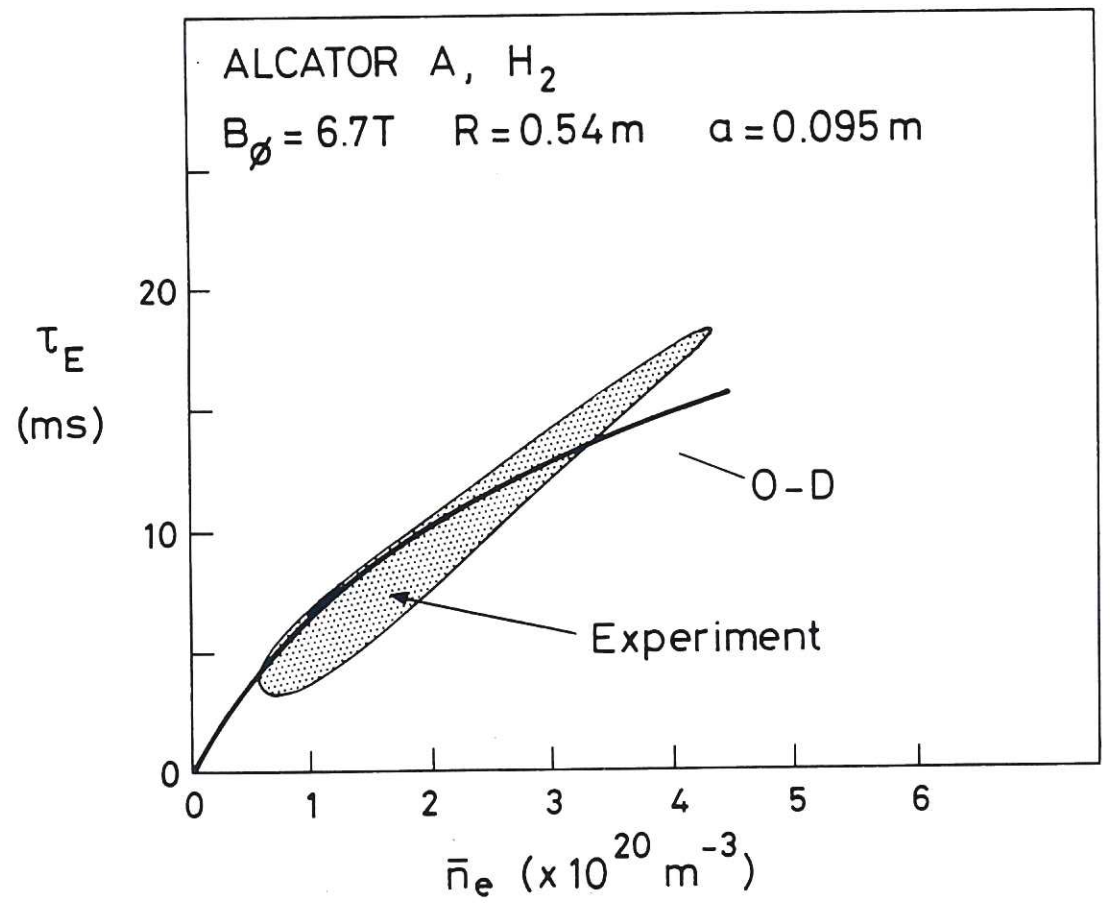

Fig.3 Comparison between experimental and calculated total energy containment times as a function of density for ALCATOR-A.

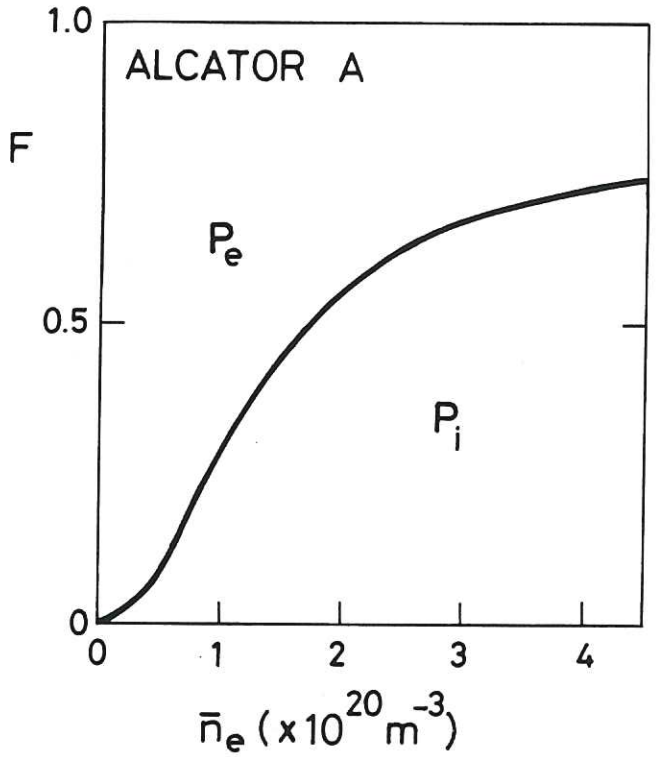

Fig.4 Fraction of power loss from the ions and electrons as a function of density for ALCATOR-A.

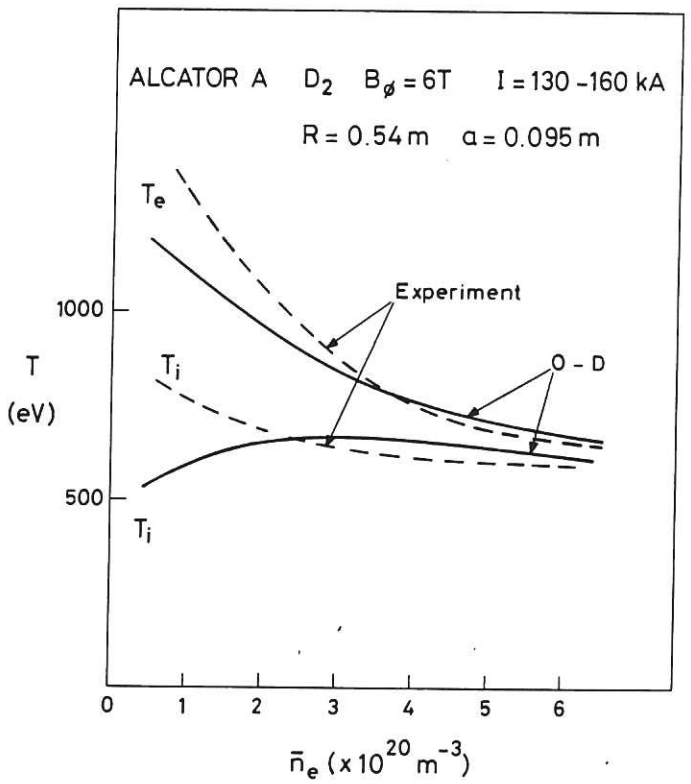

Fig.5 Calculated and experimental electron and ion temperatures as a function of electron density for ALCATOR-A.

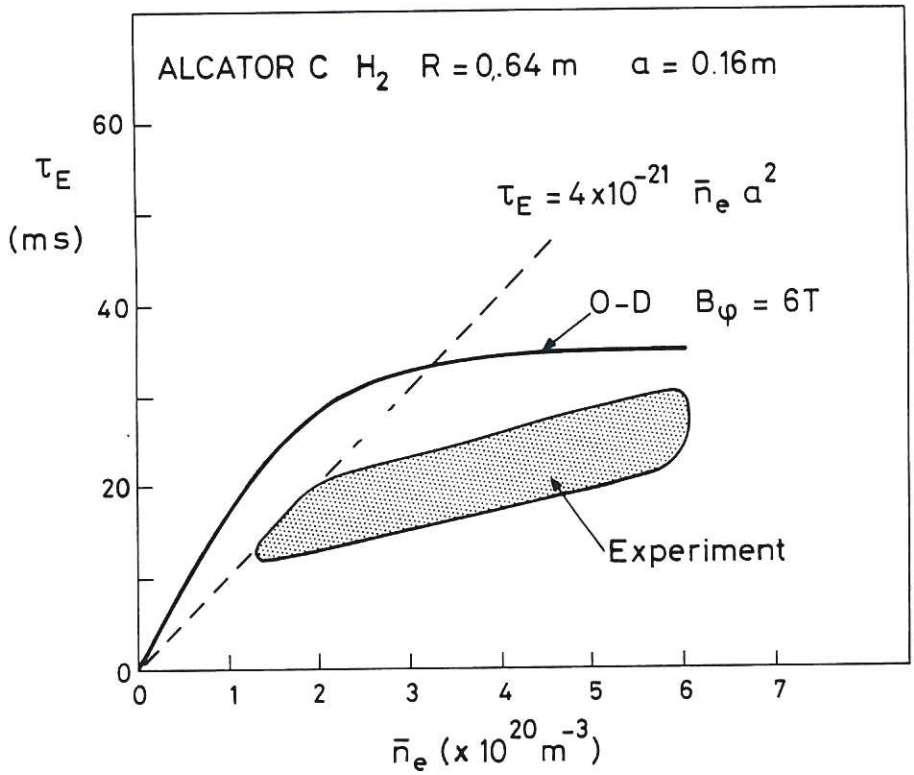

Fig.6 Calculated and experimental energy containment times for high density discharges in ALCATOR-C. The large experimental deviations from na^2 scaling are clearly reflected by the O-D model.

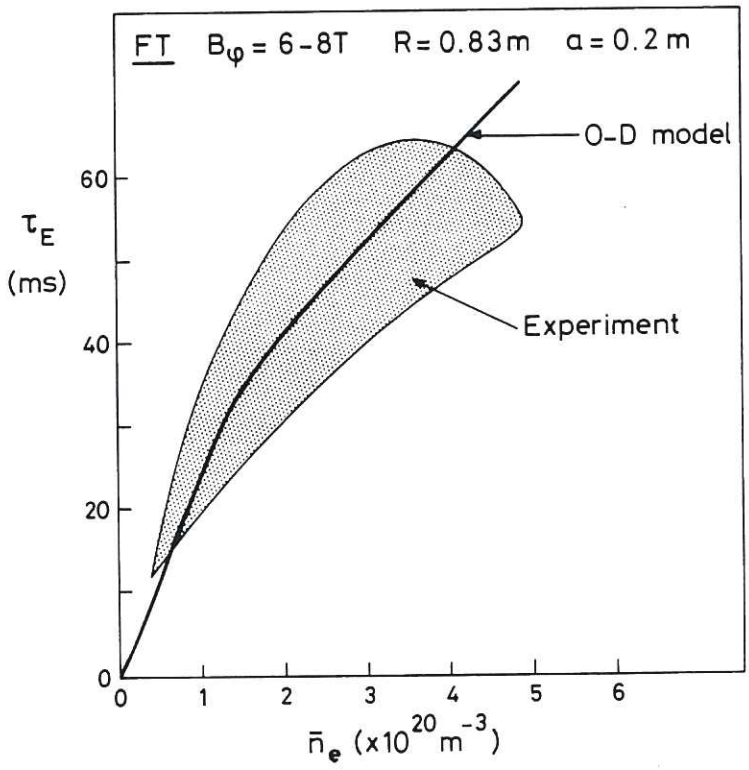

Fig.7 Energy containment time as a function of density for FT. The calculated values agree well with experiment.

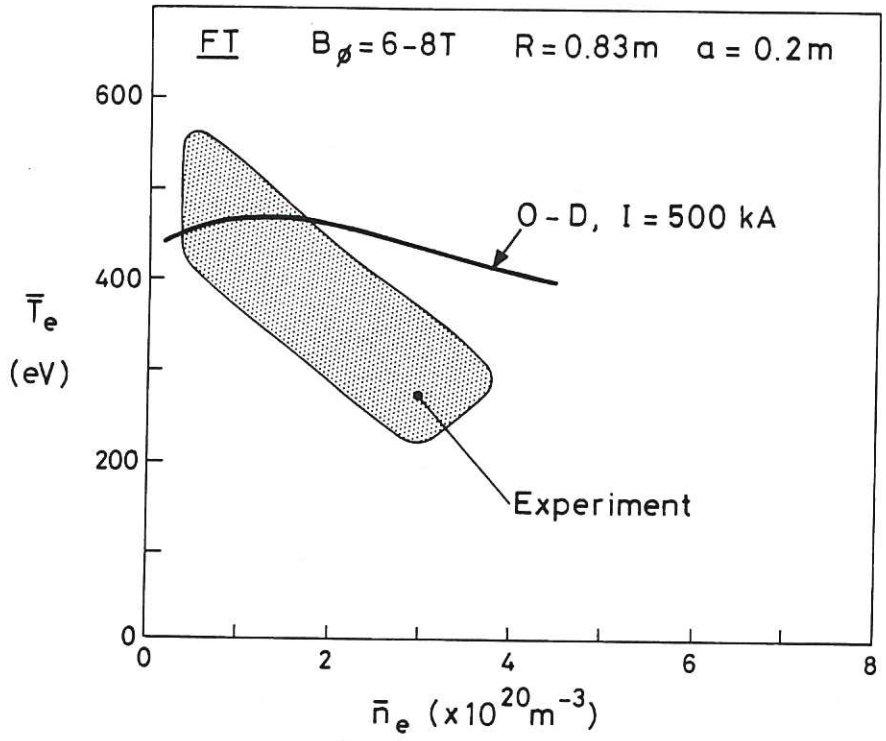

Fig.8 Mean electron temperature as a function of density for FT. The calculated values lie a little too high at high density.

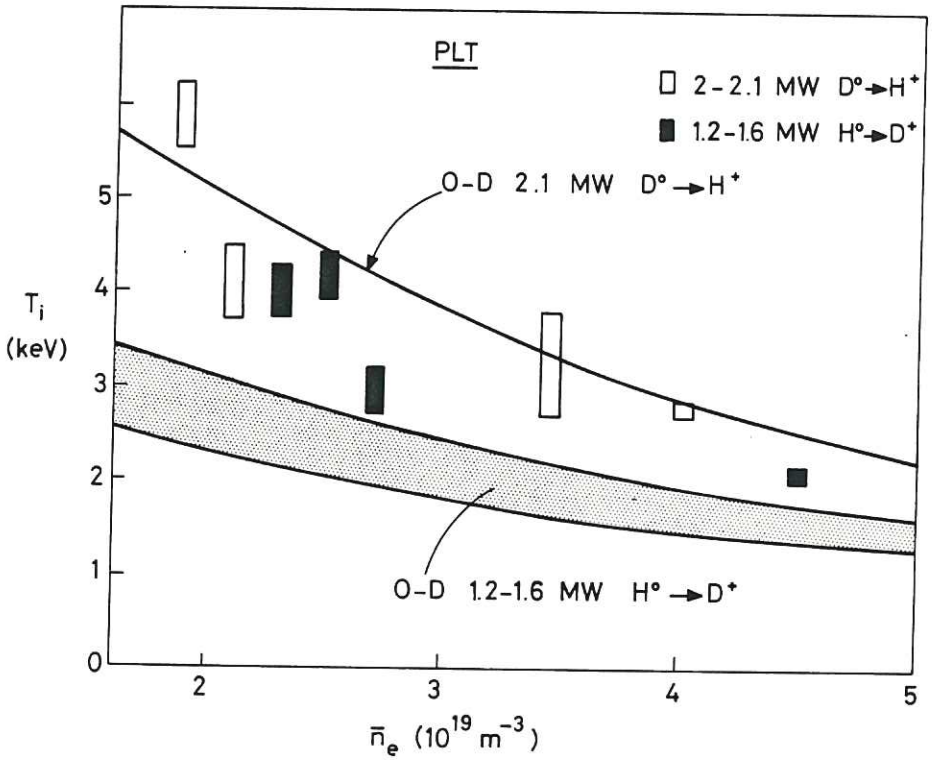

Fig.9 Ion temperature in PLT during injection heating as a function of injection power normalised by electron density.

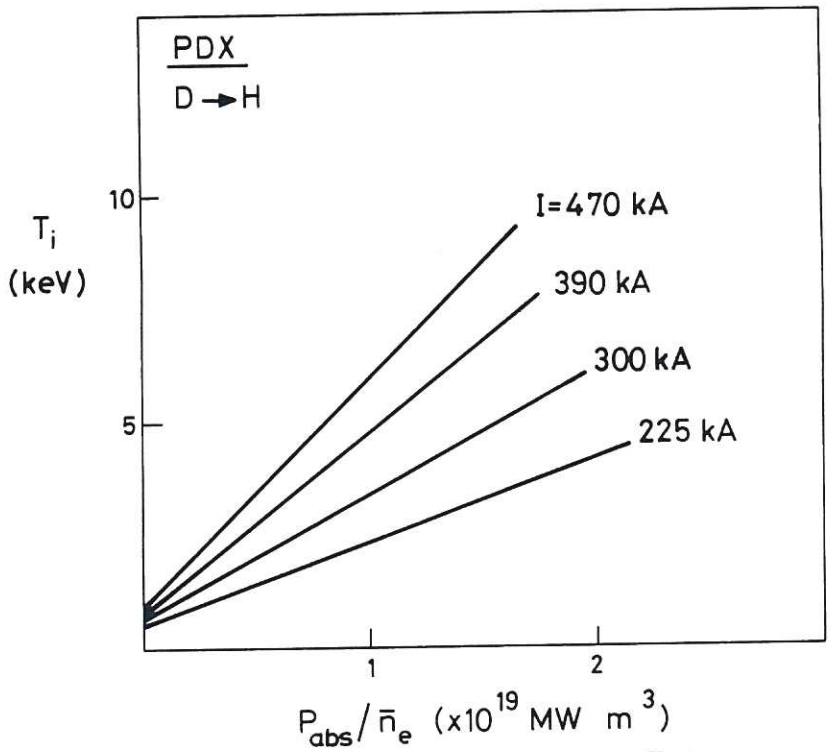

Fig.10 Ion temperature in PDX as a function of absorbed injection power normalised by density ($\bar{n}_e = 3 \times 10^{20}$ m^{-3}) for various plasma currents and for D injection into an H plasma.

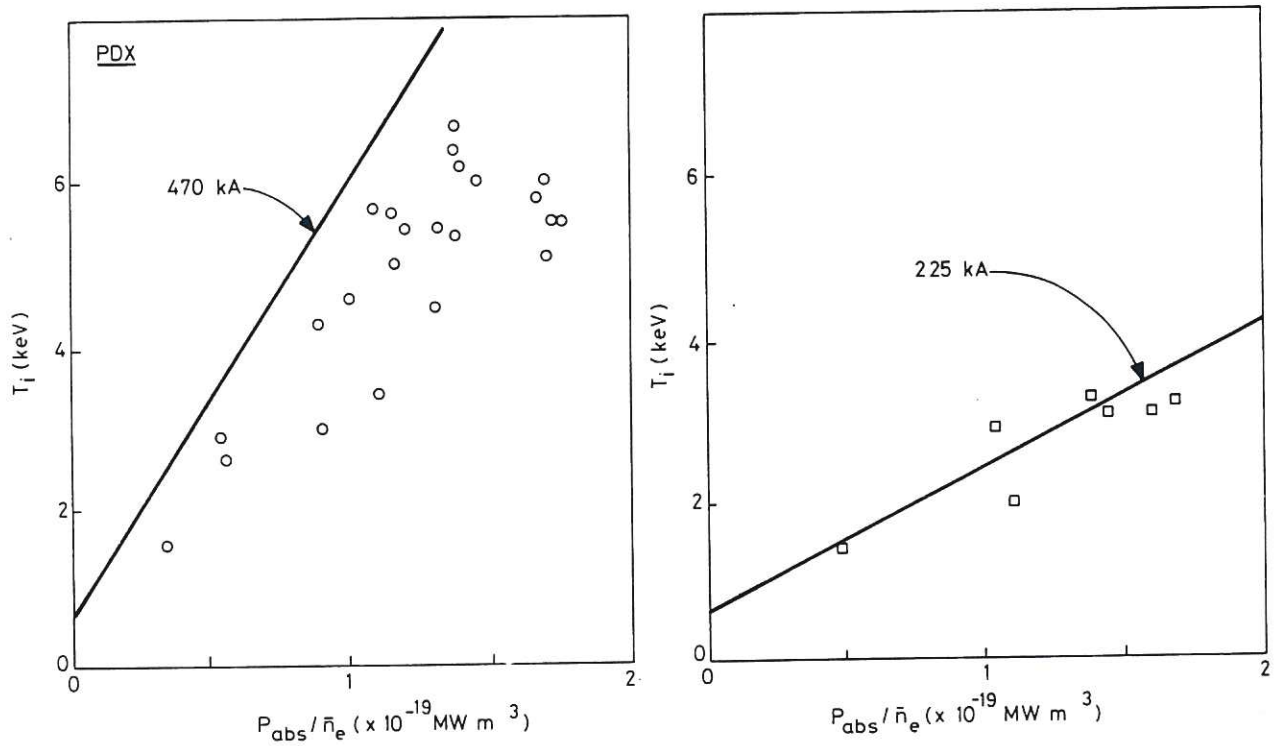

Fig.11 Comparison of calculated and experimental ion temperatures for injection of D into H plasma for two different plasma currents.

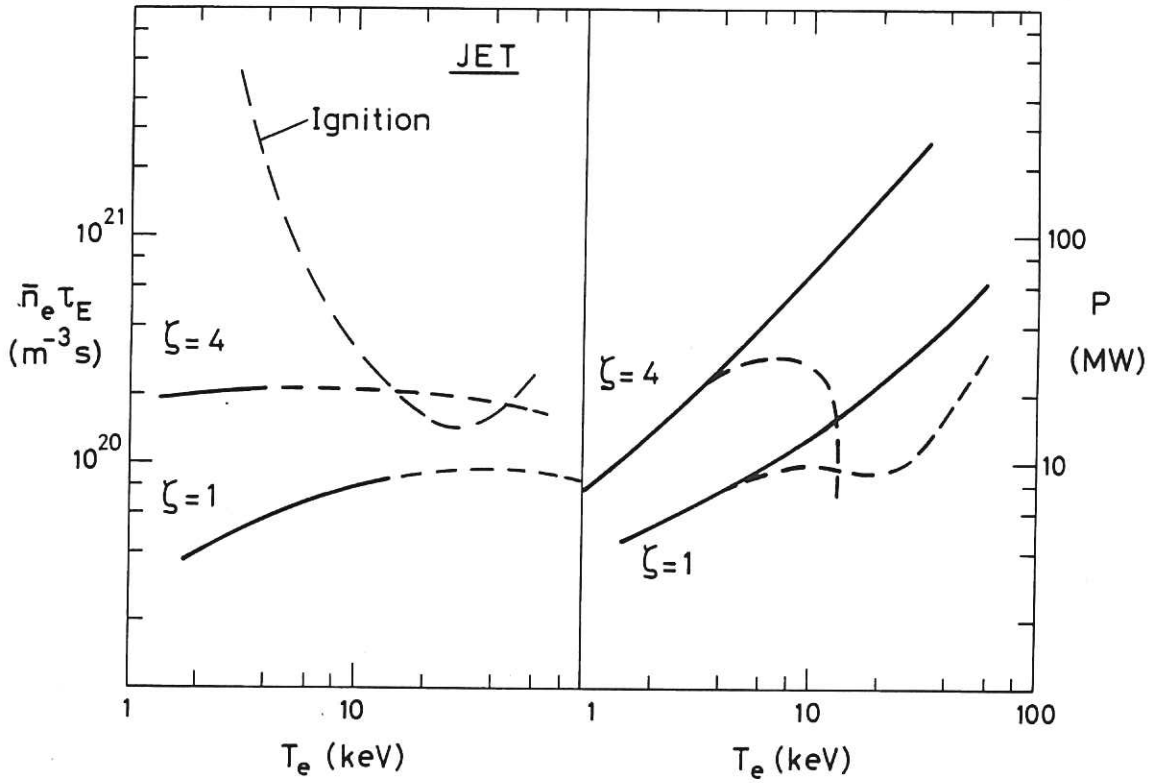

Fig.12 $n\tau$ and plasma power loss dependence on temperature for JET.

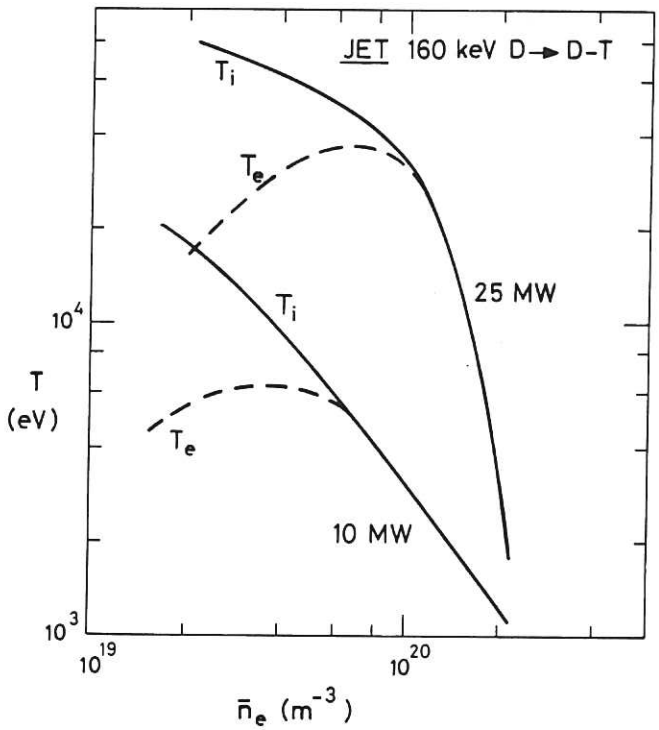

Fig.13 Electron and ion temperatures in JET as a function of density for 10 and 25MW of injection power.

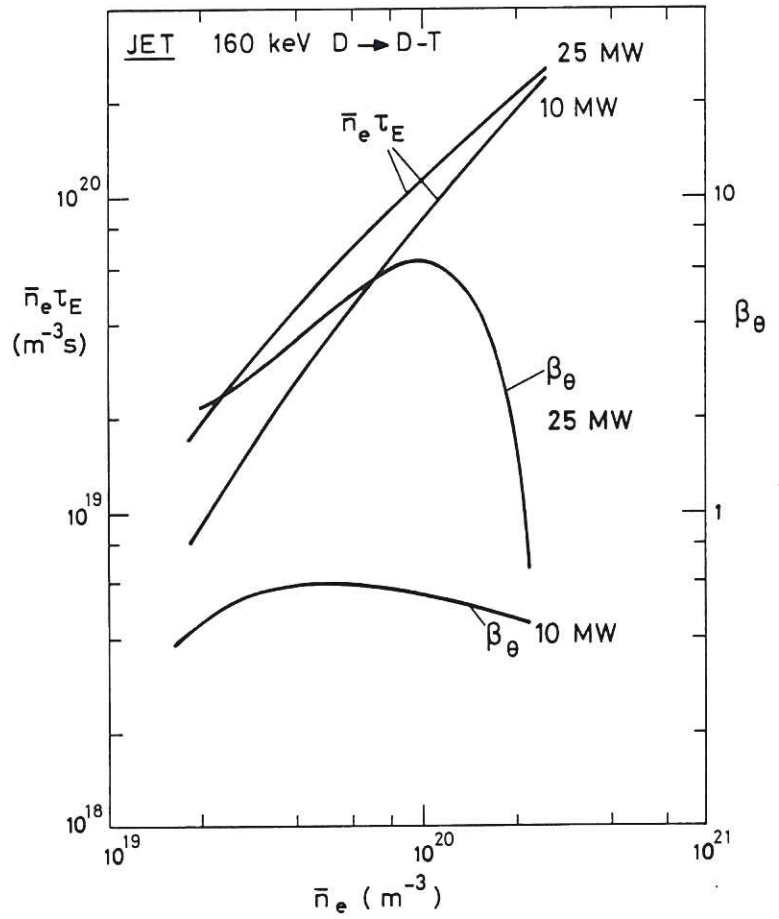

Fig.14 $n\tau$ and poloidal β versus mean electron density for 10 and 25 MW of injection power.

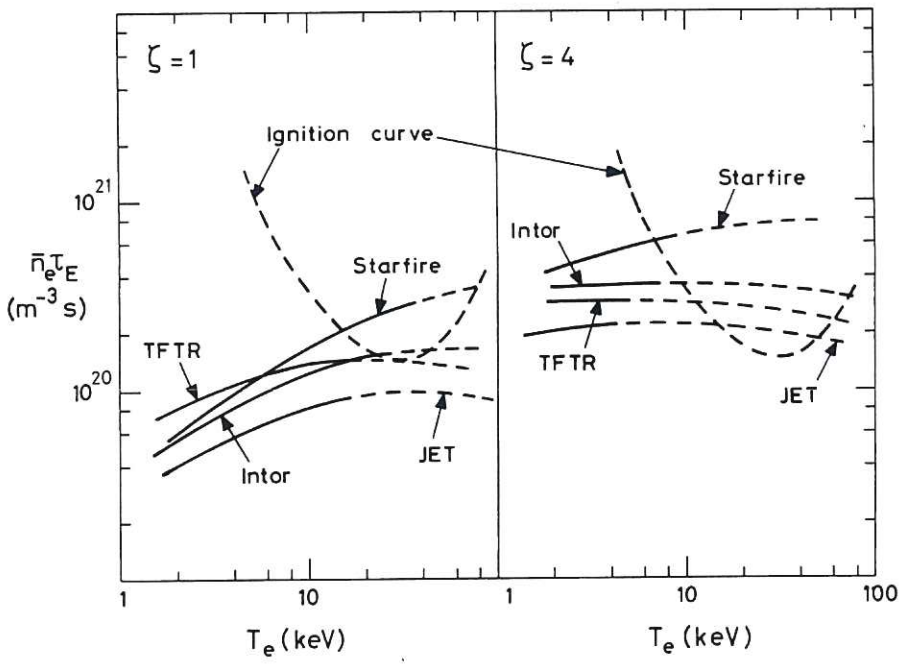

Fig.15 $n\tau$ dependence on electron temperature for a variety of machines for ζ = 1 and 4.

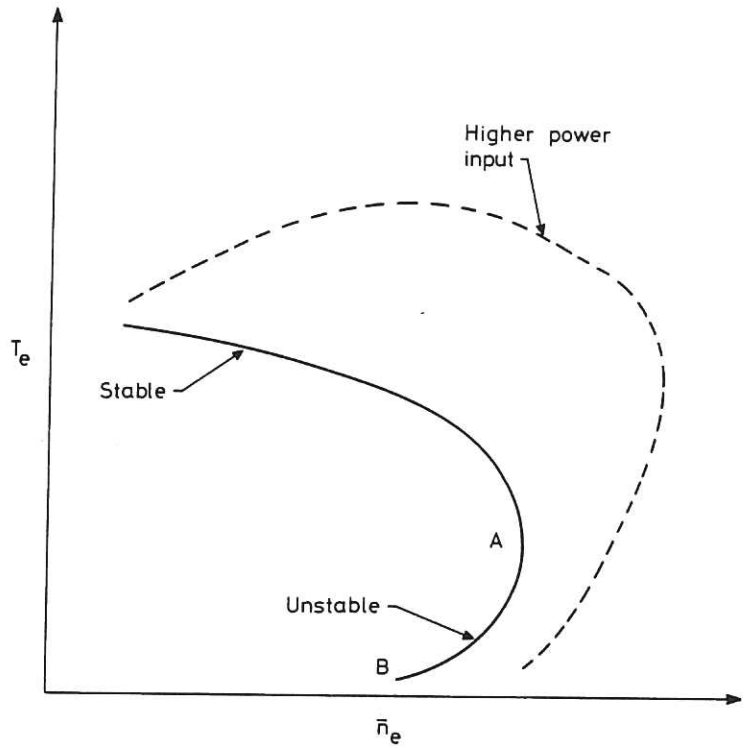

Fig.16 Schematic relationship between electron temperature and density for two levels of power input. The portion of the curve between A and B is thermally unstable so that the density at A is the maximum which can be achieved.

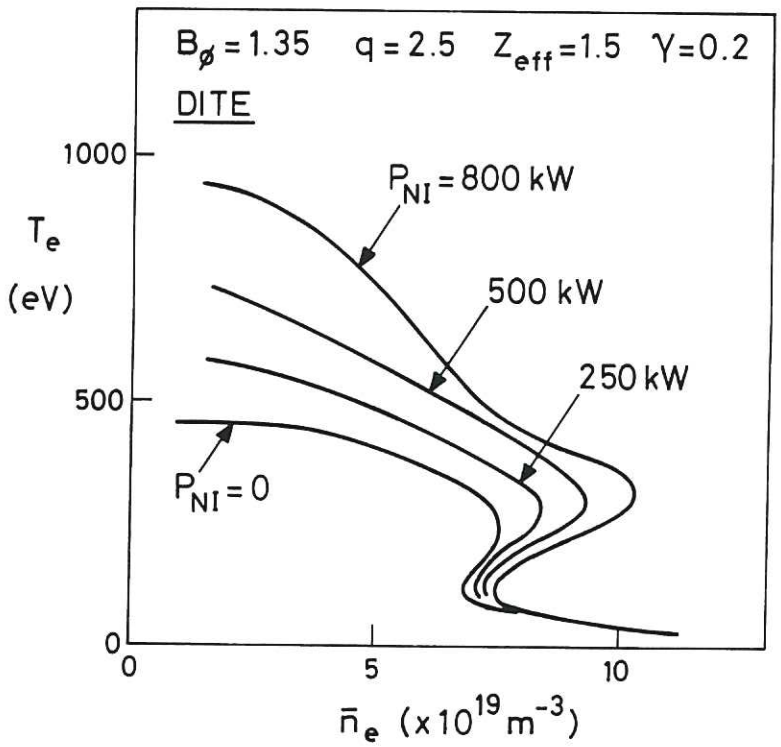

Fig.17 Calculated electron temperature versus density for various values of neutral injection power for DITE.

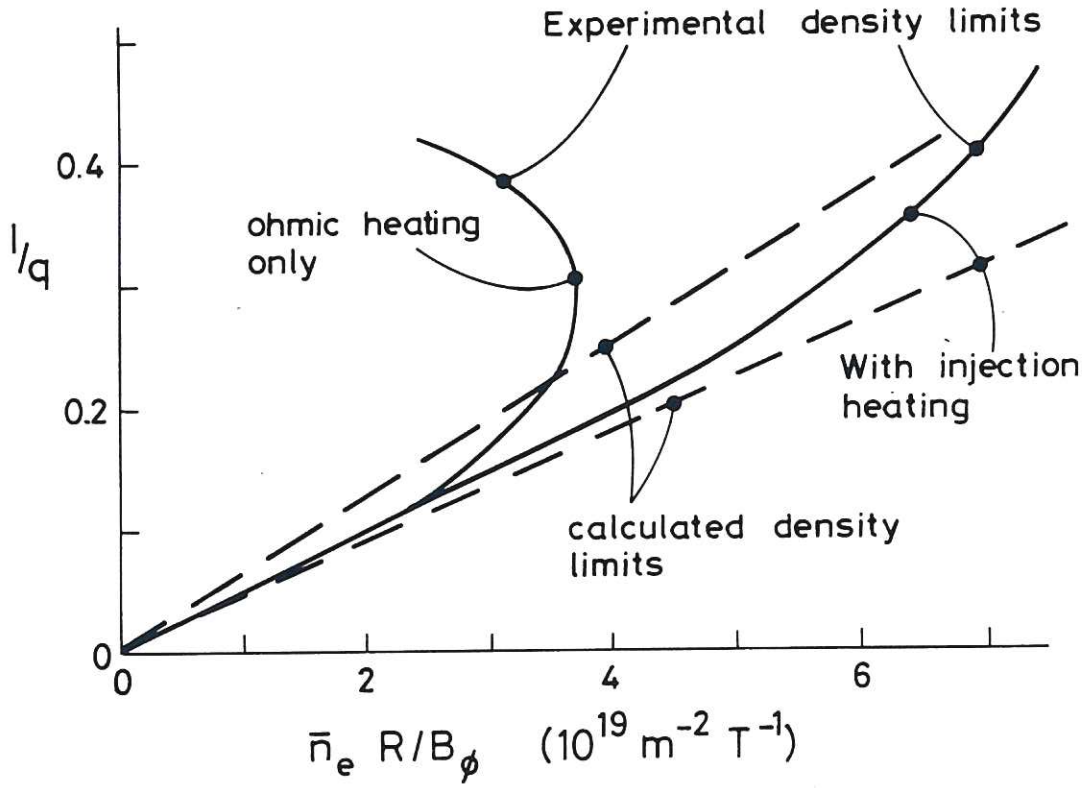

Fig.18 Calculated and experimentally determined maximum operating densities both with and without neutral injection heating in DITE.

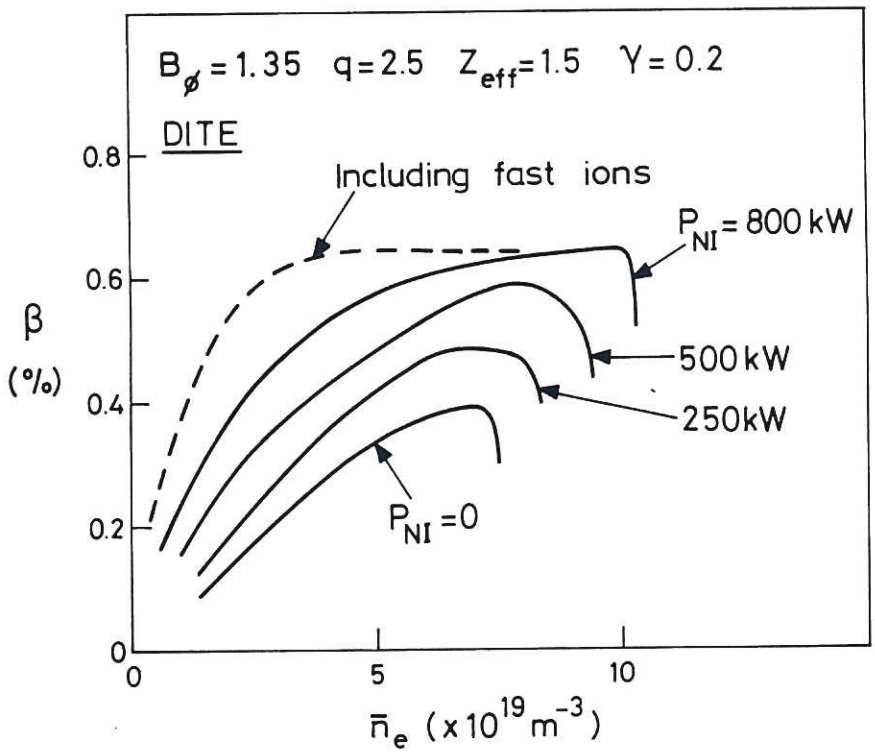

Fig.19 Plasma β as a function of density for DITE for various injection power levels. The full lines contain no contribution from the fast ions.

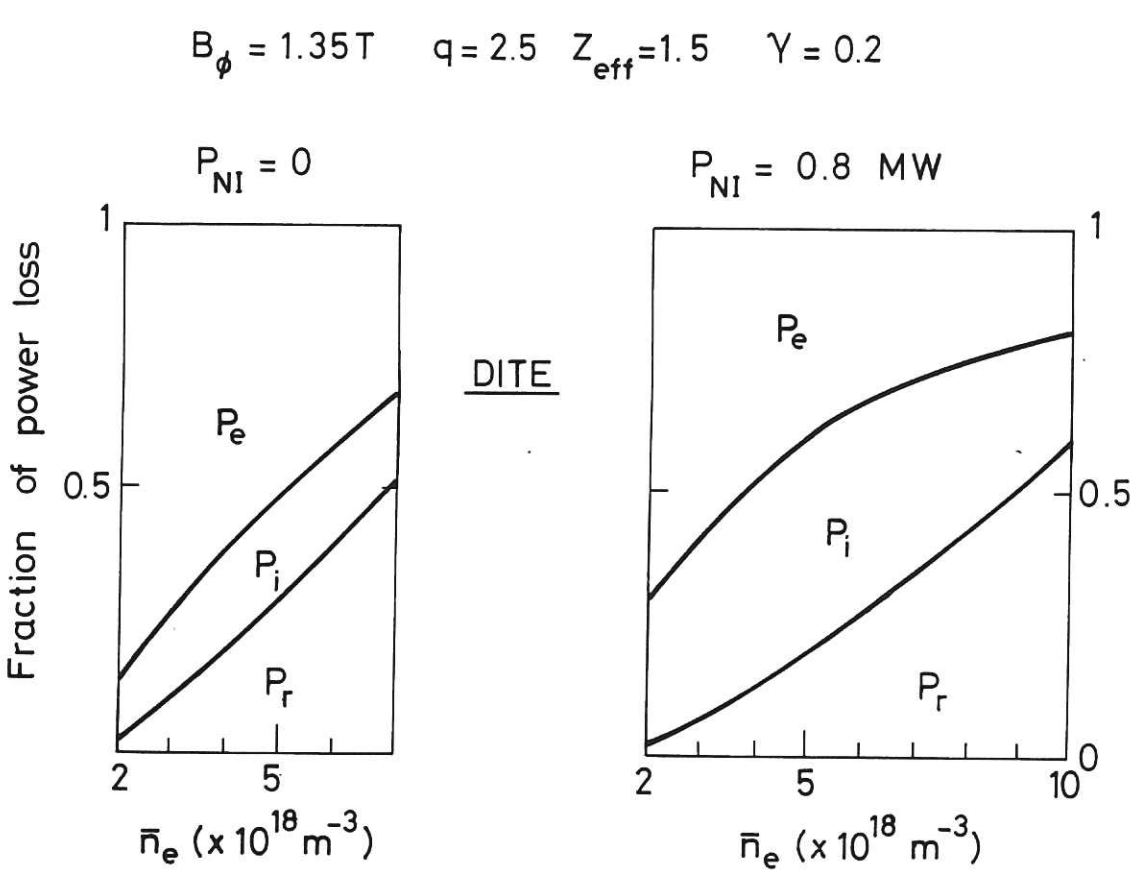

Fig.20 The fractional power lost by radiation, the ions and electrons as a function of density both with and without injection heating for DITE.

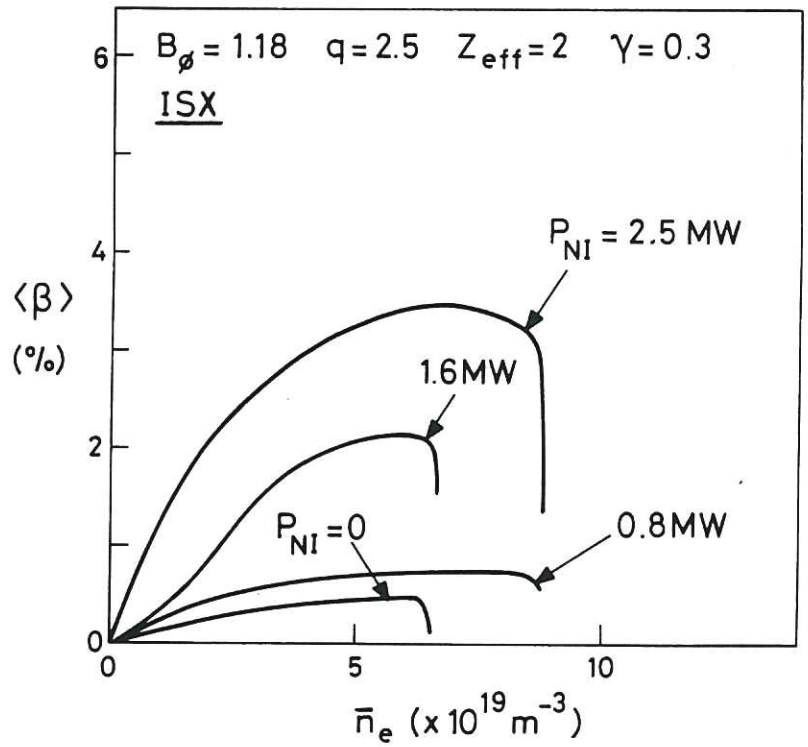

Fig.21 Mean plasma β in ISX-B calculated as a function of density for several values of injection heating power. Very clear and substantial deviations from linearity are present.

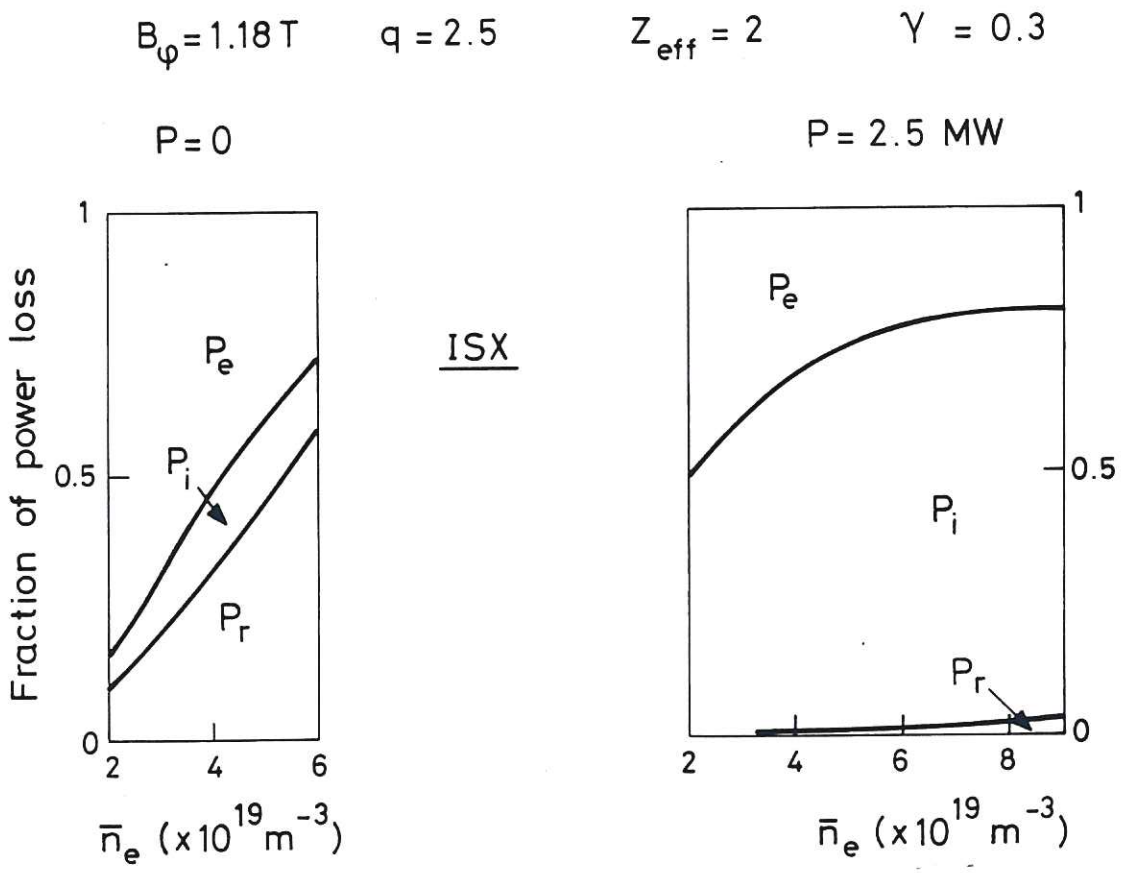

Fig.22 Power balances in ISX-B as a function of density with and without injection heating. With injection the balance is dominated by large ion losses.